

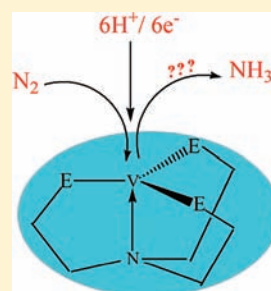
Why Vanadium Complexes Perform Poorly in Comparison to Related Molybdenum Complexes in the Catalytic Reduction of Dinitrogen to Ammonia (Schrock Cycle): A Theoretical Study

Ankur Kanti Guha and Ashwini K. Phukan*

Department of Chemical Sciences, Tezpur University, Napaam 784028, Assam, India

S Supporting Information

ABSTRACT: Energetics and mechanistic details for the conversion of dinitrogen to ammonia mediated by vanadium triamidoamine has been studied theoretically involving various mechanistic possibilities. For most of the cases, protonation at the amido nitrogen atom is more favorable compared to the terminal one. Further, the most important steps of the mechanism were compared with the well established chemistry of nitrogen fixation mediated by molybdenum. Such a comparison helps in understanding why vanadium triamidoamine complex performs poorly compared to molybdenum. The main factors responsible for the poor performance of the vanadium complex toward NH_3 production are identified as low exergonic cleavage of the N–N bond and limitation of the ligand exchange step via a dissociative mechanism at the end of the cycle to only one possible pathway. A major aspect of the failure of the vanadium complex to mediate the reduction of N_2 to ammonia is the fact that the protonation steps involve major barriers, which cannot be surmounted thermally. Moreover, unlike molybdenum, the associative mechanism with vanadium triamidoamine complex is not likely to operate during the NH_3/N_2 exchange step.



1. INTRODUCTION

The actual mechanism for the conversion of dinitrogen to ammonia by nitrogen fixing organisms is one of the unsolved problems of biology and chemistry.¹ The current phase of interest in chemical nitrogen fixation started in the early 1960s with the discovery of the first transition metal dinitrogen complex, $[\text{Ru}(\text{NH}_3)_5\text{N}_2]^{2+}$, by Allen and Senoff² and extraction of the bacterial nitrogenase in the active form.³ Also, with the revelation of the basic structure of the active site of the molybdenum nitrogenase,⁴ much of the research was devoted to the synthetic development of transition metal homogeneous catalysts for dinitrogen reduction.⁵ One such truly catalytic system for ammonia synthesis working under ambient condition is the molybdenum complex of a triamidoamine ligand, $[(\text{RNCH}_2\text{CH}_2)_3\text{N}]^{3-}$ where R = hexa-*iso*-propyl terphenyl (HIPT), synthesized by the research group of Schrock.⁶ On the basis of the isolated and characterized intermediates, they proposed a probable mechanism which was the subject of various theoretical investigations.^{7,8} Tuzek et al.^{7a} have carried out density functional calculations on the various intermediates that may appear in the catalytic cycle proposed by Schrock et al.⁶ and obtained a free energy profile for the reduction of dinitrogen to ammonia. On the basis of the energy profile so obtained which included different possible spin states of the intermediates, they concluded that the first step in the catalytic cycle is the protonation of the catalyst rather than its reduction. Reiher et al.^{8a} also carried out density functional calculations on some of the key steps of Schrock's catalytic cycle. Among them are the protonation of the $[\text{Mo}]\text{-N}_2$ ($[\text{Mo}] = [(\text{RNCH}_2\text{CH}_2)_3\text{N}]\text{Mo}$)

intermediate, dissociation of NH_3 , and addition of N_2 . Three different possibilities were considered for transfer of the first proton and electron to the coordinated N_2 intermediate. This study showed that protonation of the amido nitrogen followed by reduction and protonation to generate the neutral $[\text{Mo}]\text{-N}=\text{NH}$ molecule was thermodynamically more favorable than direct protonation of the terminal nitrogen followed by reduction. Thus, all these theoretical studies were conducted mainly on Schrock's molybdenum catalyst.

Alternative vanadium nitrogenases are now known⁹ but structurally not well characterized. In vanadium nitrogenase, the vanadium atom is thought to reside in a similar environment as the molybdenum atom in the cofactor FeMoco of Fe–Mo nitrogenase.⁹ Moreover, the catalytic efficiency of V nitrogenase in the selective formation of ammonia comes next to Mo–Fe nitrogenase. In 2006, Schrock et al.^{5k} prepared a vanadium triamidoamine complex, analogous to the molybdenum complex, and attempted the reduction of dinitrogen with this vanadium complex. They also proposed a plausible mechanism for the same. However, no ammonia was formed using this catalyst under the same condition that was successful with the analogous molybdenum catalyst. Hence, it could be rewarding to carry out a thorough theoretical investigation on the mechanism of dinitrogen fixation mediated by vanadium and to compare it with the well established chemistry of molybdenum (Scheme 1).^{6–8} To the best of our knowledge, until now, there exists no systematic

Received: April 13, 2011

Published: August 12, 2011

study in the literature about nitrogen fixation catalyzed by vanadium complexes except the one by us where mechanistic details for the conversion of hydrazine to ammonia mediated by vanadium thiolate complex were studied.¹⁰ We report here, for the first time, a systematic theoretical study on the thermodynamics of dinitrogen fixation mediated by vanadium triamidoamine complex and compared its results with the energetics obtained for the similar molybdenum complex. The key question we would like to address in this report is why vanadium complexes are not active toward NH_3 production in comparison to similar molybdenum complexes.

2. COMPUTATIONAL DETAILS

We have used density functional theory (DFT), a practical and effective computational tool, especially for transition metal compounds¹¹ for the present study. We have used the PBE1PBE¹² functional, since it performs exceedingly well for the evaluation of energetics of a reaction^{13a} as well as many other properties.^{13b} The relativistic small-core effective core potential (ECP) of Stuttgart/Dresden (SDD)^{14a} for the transition metals with the corresponding valence basis set of D95 V^{14b} for the main group elements were used. As stated by Büll et al, the combination of PBE1PBE and SDD can safely be used for studying transition metal complexes.^{13b} Frequency calculations were performed at the same level of theory to characterize the nature of the stationary points. All the ground state structures were verified as being at an energy minimum by confirming that their respective Hessian (matrix of analytically determined second order derivative of energy) led to all real valued frequencies while the transition states were characterized as stationary points with one imaginary frequency. In our calculations, the experimentally reported^{5k} hexa-*iso*-propyl terphenyl (HIPT) substituents at the amido nitrogen were modeled with hydrogen atoms so as to save computational time. In spite of this simplification, we observed an excellent agreement with the available X-ray data^{5k} (see Supporting Information, Table S1) which justifies this simplification and the level of theory used. Moreover, replacement of the bulky HIPT group by hydrogen does not change the nature of the reaction, although quantitative differences are observed (see Supporting Information, Table S2). Energies corresponding to the reduction and protonation steps were calculated relative to the process $[\text{Cp}^*_2\text{Cr}] \rightarrow [\text{Cp}^*_2\text{Cr}]^+ + e^-$ and $\text{LutH}^+ \rightarrow \text{Lut} + \text{H}^+$ (Lut = 2,6-dimethylpyridine), without making any simplifications of the molecules involved. Zero-point energy (ZPE), thermal, as well as solvent (heptane) corrections, was employed in computing the standard free energies of formation. The bonding nature of all the compounds was analyzed by natural bond orbital (NBO) analysis.¹⁵ All the computations were performed using the Gaussian 03

Scheme 1

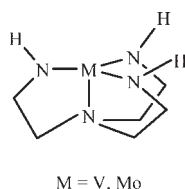


Table 1. Charge Decomposition (CDA) Analysis of $[\text{V}]\text{-N}_2$ and $[\text{Mo}]\text{-N}_2$ Complexes Calculated at the PBE1PBE/SDD Level of Theory along with NBO Occupancies of the Two Orthogonal π^* Orbitals of $\text{N}\equiv\text{N}$ in Their Respective Complexes^a

complex	$\text{N}_2 \rightarrow \text{M}$ donation (<i>d</i>)	$\text{M} \rightarrow \text{N}_2$ back-donation (<i>b</i>)	<i>b/d</i>	repulsion (<i>r</i>)	residue (Δ)	occupancy of $\pi^*_{\text{N}\equiv\text{N}}$	ν_{NN} (cm^{-1})
$[\text{Mo}]\text{-N}_2$	0.217	0.339	1.562	-0.325	-0.033	0.169/0.184	1894.8
$[\text{V}]\text{-N}_2$	0.234	0.264	1.128	-0.164	-0.066	0.136/0.125	2090.4

^a ν_{NN} (cm^{-1}) is the infrared N_2 stretching frequency (without scaling).

program,¹⁶ while the charge decomposition analysis (CDA)¹⁷ was performed using the QMForge 2.1 program.¹⁸

3. RESULTS AND DISCUSSION

3.1. Mechanistic Details of $[\text{V}]$ ($[\text{V}] = (\text{N}_3\text{N})\text{V}$). Dinitrogen binding to a transition metal center is crucial as it activates the strong $\text{N}\equiv\text{N}$ bond. The interaction involves donation of electron density from the filled orbital of the Lewis base N_2 into the empty metal orbital (d_{z^2}) resulting in the formation of a σ -bond. The filled metal orbital (d_{xy} and d_{xz}) on the other hand back-donates electron density to the lowest unoccupied orbital of N_2 resulting in the formation of a π back-bond. The extent of back-donation from the metal center is responsible for the activation of the $\text{N}\equiv\text{N}$ bond as electron density from the filled metal orbital enters into the antibonding orbital of N_2 of appropriate symmetry. The CDA of Frenking et al.¹⁸ helps in analyzing such a situation (Table 1). Since the residue terms (Δ) are nearly zero, the metal- N_2 interaction can be discussed within the framework of the familiar Dewar–Chatt–Duncanson donor–acceptor model.¹⁹ The values of back-donation (*b*) from the metal center to the π^* orbital of N_2 and the ratio *b/d* are found to be higher for the $[\text{Mo}]$ catalyst compared to $[\text{V}]$. Hence, $[\text{Mo}]$ is more efficient in activating the $\text{N}\equiv\text{N}$ bond compared to $[\text{V}]$ ($r_{\text{N}\equiv\text{N}} = 1.200 \text{ \AA}$ and 1.141 \AA in $[\text{Mo}]\text{-N}_2$ and $[\text{V}]\text{-N}_2$, respectively). Infrared N_2 stretching frequencies (without scaling) as well as the occupancies of the two orthogonal π^* orbitals of $\text{N}\equiv\text{N}$ also show the same trend, that is, $[\text{Mo}]\text{-N}_2$ has higher occupancies of the two π^* orbitals of $\text{N}\equiv\text{N}$ and thus, has lower N_2 stretching frequency. Hence, CDA and Natural Bond Orbital (NBO)¹⁵ results show that the degree of dinitrogen activation is higher with $[\text{Mo}]$ compared to $[\text{V}]$. However, several controlled studies have revealed that the degree of dinitrogen activation and the extent of reactivity may not always correlate.²⁰

The most crucial steps in the initial stage of the mechanism are the addition of dinitrogen followed by its successive protonation and reduction. Figure 1 shows three possible pathways of dinitrogen addition, protonation, and reduction. According to the energy profile obtained at the PBE1PBE/SDD level of theory, path C, which is the addition of dinitrogen to the neutral $[\text{V}]$ catalyst followed by subsequent protonation and reduction to yield $[\text{V}]\text{-N}=\text{NH}$, is the most preferred pathway of the three possibilities shown in Figure 1. The high energetic barrier of path B, which involves reduction of $[\text{V}]$ prior to the addition of dinitrogen makes it least likely. This is in tune with Tuzek's mechanism where protonation of the coordinated dinitrogen takes place prior to reduction.^{7a} The slightly more endergonic character of path A compared to C also makes this path less likely. Further, the proton may attach either to the terminal nitrogen, N_β , of the dinitrogen ligand, or it can attach to the amido nitrogen atom, N_{eq} . Therefore, we have also checked this possibility as shown in Figure 2. The computed energy profile shows that protonation at amido nitrogen, N_{eq} , resulting in the formation of $[\text{V}\text{-N}_{\text{eq}}\text{H}]\text{-N}_2^{\dagger+}$, is nearly 60 kcal/mol more

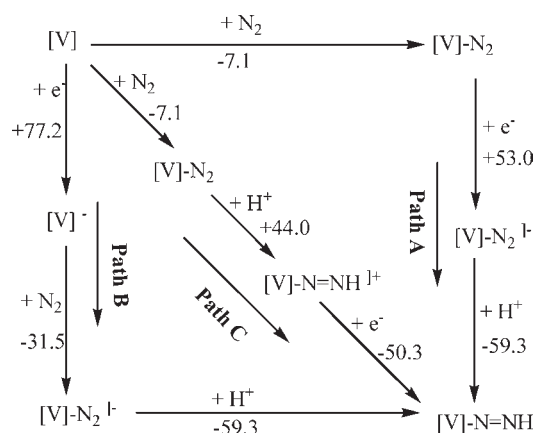


Figure 1. Three possible pathways of dinitrogen addition, protonation, and reduction of $[V]$ ($[V] = (N_3N)V$) to yield $[V]-N=NH$. Energies are in kcal/mol.

favorable compared to protonation at N_β . More negative charge at N_{eq} (-0.97) compared to N_β (0.05) favors protonation at N_{eq} . Similar energetics were obtained by Reiher et al.^{8a} for protonation at amido and terminal nitrogen atoms of the related $[Mo]$ complex. Using a combination of electron paramagnetic resonance (EPR) and electron nuclear double resonance (ENDOR) spectroscopy and DFT computations, Schrock and co-workers have recently shown that the incoming proton preferentially binds to the amido ligand (i.e., one of the equatorial nitrogen atoms) prior to its eventual migration to the N_β of N_2 .²¹ The protonated molecule $[V-N_{eq}H]-N_2^{1+}$ then undergoes reduction to produce $[V-N_{eq}H^+]-N\equiv N^-$ which is exergonic by 30.2 kcal/mol. The resulting complex then undergoes protonation at the N_β position to produce $[V-N_{eq}H^+]-N=NH$ which on further deprotonation, produces $[V]-N=NH$. Thus, it is evident from Figure 2 that protonation at the amido position is much more favorable than at the terminal one to produce $[V]-N=NH$ and is “proton catalyzed”. This is in tune with previous theoretical and experimental results for the analogous $[Mo]$ complexes.^{6f,8a,8b,21} On the basis of the above observations, a mechanism has been proposed, and its corresponding standard free energies have been calculated and plotted in Figure 3 against the reaction coordinate ρ .

The starting complex **1**, $[V]$ ($[V] = (N_3N)V$), is a trigonal monopyramidal complex which gives rise to $S = 0$ and $S = 1$ states. The singlet-triplet energy separation of **1** is 37.8 kcal/mol, with the triplet state being more stable. Addition of neutral N_2 results in an end on bound dinitrogen complex $[V]-N_2$ (**2**) with triplet ground state (the singlet state lies 26.2 kcal/mol higher in energy than the triplet state). This addition is found to be exergonic by an amount of 7.1 kcal/mol. The next step is a crucial one which involves protonation of the coordinated dinitrogen complex. As evident from Figure 2, protonation of the coordinated dinitrogen complex is more favorable at the amido position rather than at N_β , to form $[V^{III}-N_{eq}H]-N_2^{1+}$ (**3**) with triplet ground state (the singlet state is 29.8 kcal/mol higher in energy than the triplet state). This protonation process is exergonic by 15.9 kcal/mol. The resulting protonated dinitrogen complex then undergoes reductive proton migration to N_β via a “proton catalyzed” pathway (Figure 2) resulting in the formation of $[V^{IV}-N=NH]$ (**4**) with doublet ground state. This process is endergonic by 9.5 kcal/mol. Interestingly, the reductive proton

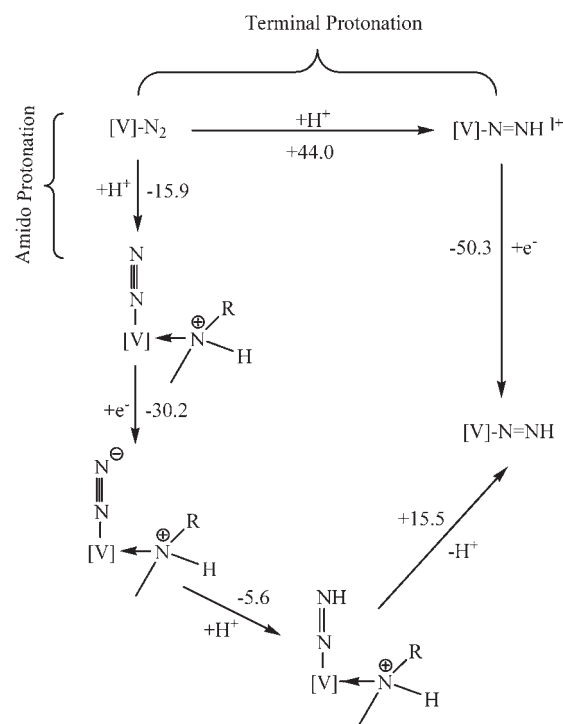


Figure 2. Two possibilities for the initial protonation (amido and terminal) of $[V]-N_2$ ($R = H$). Energies are in kcal/mol.

migration step for the related molybdenum complex is exergonic by 22.4 kcal/mol. Since the conversion of **3** to **4** involves a barrier of 9.5 kcal/mol, we decided to look for any possible intermediate or transition state for this conversion (Figure 4). We could locate an intermediate **3I** which is formed via 1,2 proton shift from the amido nitrogen to the vanadium atom during the reduction of **3**. The N_2 moiety in **3I** is tilted away from the axis defined by the N_b-V-N_α (N_b is the bridgehead nitrogen atom) atoms making an angle of 155.3° at the vanadium center. The formation of this intermediate is calculated to be endergonic by 13.5 kcal/mol. The intermediate **3I** then rearranges to **4** via a transition state **TS-I** in which the proton migrates from the vanadium center to the terminal nitrogen atom. The barrier height for the conversion of **3I** \rightarrow **4** is calculated to be +17.8 kcal/mol. Thus, transformation of **3** to **4** may involve one probable intermediate **3I** and a transition state **TS-I**.

As in the case of first protonation, complex **4** then undergoes further protonation at the amido nitrogen atom (for a comparison of amido versus terminal protonation, see Supporting Information, Table S3) to form $[V^{IV}-N_{eq}H]-N=NH^{1+}$ (**5**) with no change in multiplicity. This process is exergonic by 13.2 kcal/mol. The next step is the reductive proton migration of the cationic complex **5** to form the neutral complex $[V^V]=N-NH_2$ (**6**) with singlet ground state (the triplet state is 15.1 kcal/mol higher in energy than the singlet state) and may proceed via a “proton catalyzed” pathway as observed in the case of the **2** \rightarrow **4** conversion (Figure 2). Such proton catalyzed pathways are not considered for other protonation steps, but instead, only the protonation at the amido nitrogen and its reductive proton migration to terminal N_β position are considered. The conversion of **5** to **6** is exergonic by 26.2 kcal/mol. Protonation of **6** at the amido nitrogen is favorable by 28.1 kcal/mol compared to terminal protonation (see Supporting Information, Table S3)

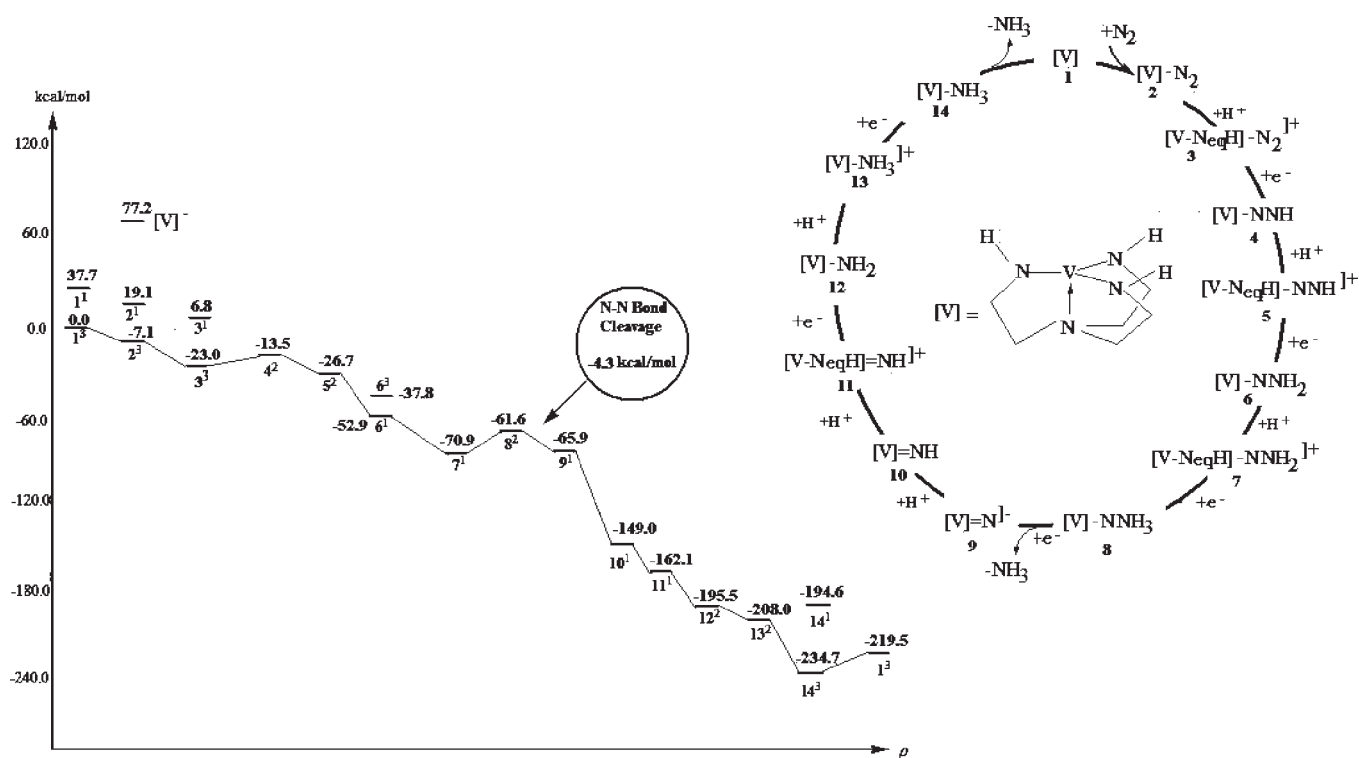


Figure 3. Catalytic cycle (top right) and free energy profile for the reduction of N₂ to ammonia mediated by [V] ([V] = (N₃N)V) systems. Energies correspond to standard free energies of formation (ΔG^0) and are in kcal/mol. Energies shown are not to scale.

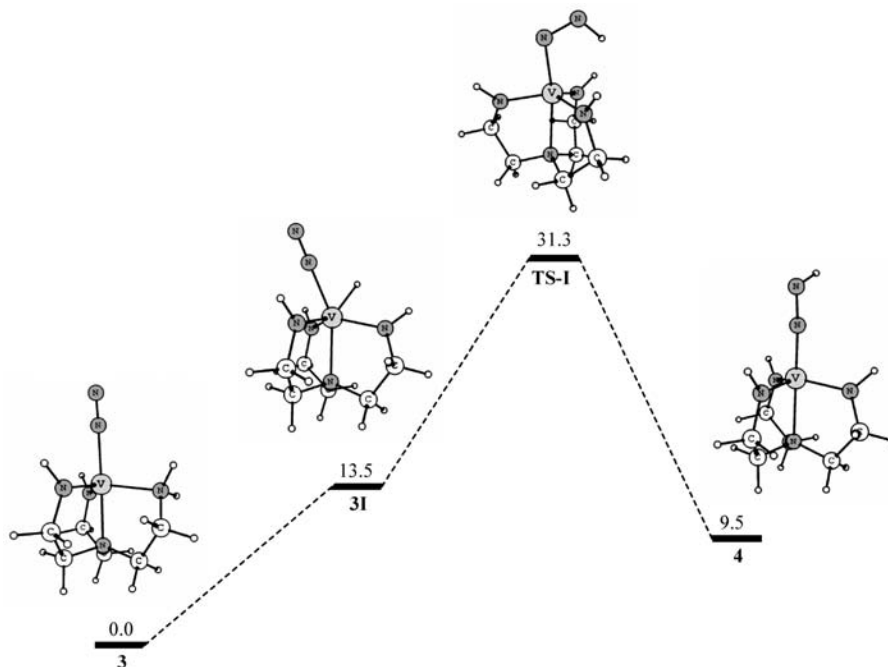


Figure 4. Possible intermediate and transition state for the conversion of 3 to 4. Energies correspond to standard free energies of formation (ΔG^0) and are in kcal/mol.

and results in the formation of the cationic complex $[V^V-N_{eq}H]-NNH_2^{1+}$ (7) with no change in multiplicity and is exergonic by 18.0 kcal/mol. The reductive proton migration of 7 results in the formation of the neutral complex $[V]^{IV}-NNH_3$ (8)

with a doublet ground state. Since the conversion of 7 to 8 also involves an energetic barrier of 9.4 kcal/mol as in the conversion of 3 \rightarrow 4, we decided to look for any possible intermediate or transition state that may form during this transformation as well

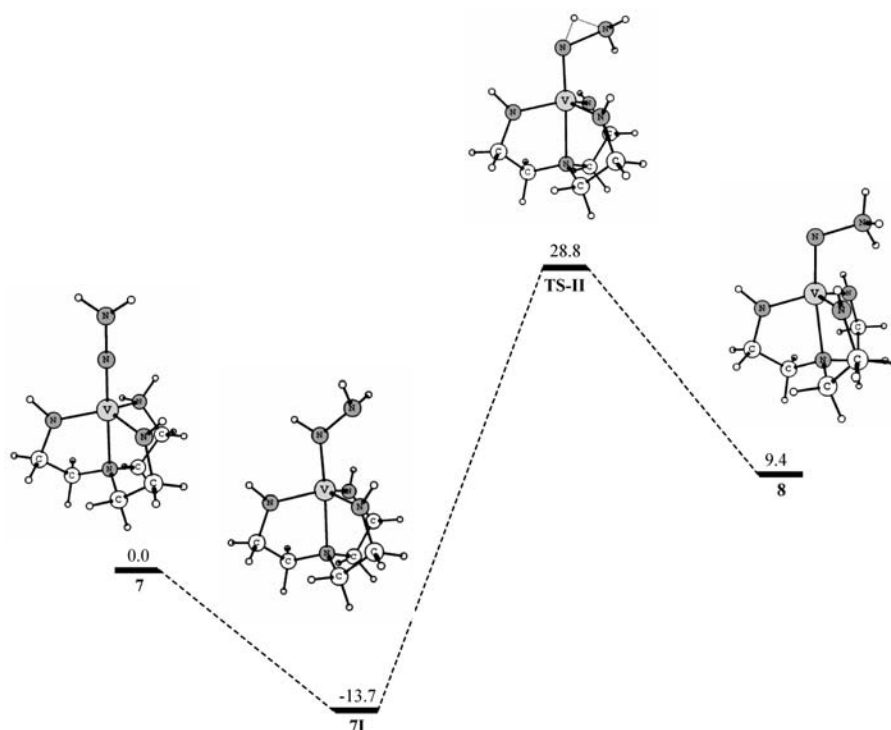


Figure 5. Possible intermediate and transition state for the conversion of **7** to **8**. Energies correspond to standard free energies of formation (ΔG^0) and are in kcal/mol.

(Figure 5). We could locate an intermediate **7I** which is formed via 1,3 proton shift from the amido nitrogen to the N_α atom. The formation of this intermediate is found to be exergonic by 13.7 kcal/mol. It then rearranges via 1,2 shift to produce **8** via a transition state **TS-II** which lies 42.5 kcal/mol higher in energy than **7I**. However, as proton transfer reactions are very fast because of the high tunneling ability of the proton, these intermediates as well as the transition state may not be observed experimentally.

The next step is a key one which involves the generation of the first equivalent of ammonia. It involves reduction of the neutral complex **8** to yield the anionic complex $[V]^V=N^-$ (**9**) with subsequent generation of the first equivalent of ammonia. The N–N bond in **8** is highly activated as is evident from the large N–N distance of 1.535 Å compared to 1.098 Å in free N_2 .²² This activation of the N–N bond facilitates its exergonic cleavage which is calculated to be 4.3 kcal/mol. In principle, such activated N–N bond should have resulted in a highly exergonic cleavage of the N–N bond and facile release of NH_3 . The fact that release of NH_3 is not so facile (exergonic by only 4.3 kcal/mol), further lends support to the observation that the degree of nitrogen activation and the extent of reactivity may not always correlate.²⁰

The next two steps are the protonation of **9** to produce the neutral complex $[V]^V=NH$ (**10**) with subsequent protonation of **10** to produce the cationic complex $[V^V-N_{eq}H]=NH^{1+}$ (**11**) with no change in multiplicity. For simple electrostatic reason, protonation of **9** is more favorable at the terminal nitrogen atom rather than the amido one (see Supporting Information, Table S3). However, protonation of **10** is more favorable at the amido nitrogen atom. These two protonation steps are found to be exergonic (Figure 3) with the first one, that is, **9** \rightarrow **10** being highly exergonic by 83.1 kcal/mol. Reduction of **11** yields the neutral complex $[V]^{IV}-NH_2$ (**12**) with a doublet ground state.

This reduction process was calculated to be exergonic by 33.3 kcal/mol. The next step is the protonation of the neutral complex **12** to yield $[V]^{IV}-NH_3^{1+}$ (**13**) with no change in multiplicity. The protonation of **12** at the terminal and amido nitrogen atoms proceeds with almost equal probability (see Supporting Information, Table S3) and hence, the terminal protonated molecule **13** is retained in the mechanism. This protonation is found to be exergonic by 12.6 kcal/mol. The next step is the reduction of the cationic complex **13** to the neutral $[V]^{III}-NH_3$ complex (**14**) with triplet ground state (the singlet state is 40.1 kcal/mol higher in energy than the triplet state), and is calculated to be exergonic by 26.7 kcal/mol. The last step is an important one where regeneration of the catalyst and production of second equivalent of ammonia takes place. This process is found to be endergonic by an amount of 15.2 kcal/mol.

It can be seen from Figure 3 that whenever there is a possibility for more than one spin state, the high spin geometry lies lower in energy than the low spin one except in case of $[V]=N-NH_2$ (**6**) where the high spin (triplet) state lies 15.1 kcal/mol higher in energy than the low spin (singlet) state. Also, in agreement with experimental findings by the group of Schrock,^{5k} we find that the conversion of $[V]=NH$ (**10**) to $[V]-NH_3$ (**14**) via $[V]-NH_2$ (**12**) is quite facile.

3.2. Comparison between [V] and [Mo] Catalyst. Since no ammonia was generated using the [V] catalyst under the same condition that was successful for the analogous [Mo] catalyst,^{5k} we therefore decided to investigate the factors which might be responsible for the lower activity of the [V] catalyst. It is clear from Figure 3 that the key steps for the generation of ammonia are (i) N–N bond cleavage along with the generation of the first equivalent of NH_3 (process **8** \rightarrow **9**) and (ii) release of the second molecule of NH_3 and regeneration of the catalyst (process **14** \rightarrow **1**).

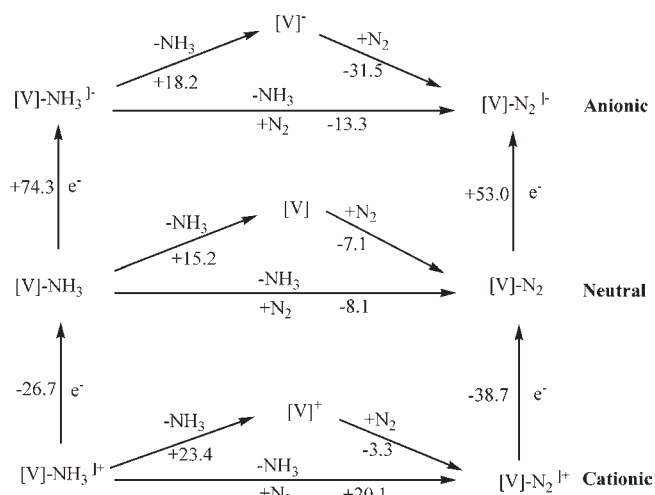


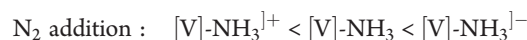
Figure 6. Different possibilities of initial NH₃/N₂ exchange. Energies are in kcal/mol.

The N–N bond cleavage step is found to be exergonic by only 4.3 kcal/mol. However, the N–N bond cleavage step with [Mo] is found to be exergonic by 75.9 kcal/mol at the same level of theory (see Supporting Information). To understand the origin of such a large difference in energetics, one has to look at the energies of the σ antibonding orbital of the N $_{\alpha}$ -N $_{\beta}$ bond of the isoelectronic d¹ species [V]-NNH₃ and [Mo]-NNH₃¹⁺ respectively as NH₃ will be released from these molecules upon reduction. It is found that the $\sigma^*_{N_{\alpha}-N_{\beta}}$ orbital of [V]-NNH₃ lies 2.4 eV higher in energy than that for [Mo]-NNH₃¹⁺ (energies of $\sigma^*_{N_{\alpha}-N_{\beta}}$ for [V]-NNH₃ and [Mo]-NNH₃¹⁺ are 4.1 and 1.7 eV respectively, Supporting Information, Figure S1). Thus, the molybdenum complex more readily undergoes reduction than the vanadium one, and hence, N–N bond cleavage and subsequent release of NH₃ is highly exergonic in this case. However, because of the much higher energy of the $\sigma^*_{N_{\alpha}-N_{\beta}}$ orbital of the vanadium complex, it is quite difficult to reduce the N $_{\alpha}$ -N $_{\beta}$ bond. It is this difficulty in reducing the N $_{\alpha}$ -N $_{\beta}$ bond which is responsible for the significantly less exergonic cleavage of the N $_{\alpha}$ -N $_{\beta}$ bond, and this account for the inefficient release of NH₃ from the vanadium complex compared with that in the related molybdenum complex. Also, the natural charge at the vanadium atom of [V]-N-NH₃¹⁺ is 0.90e while that of molybdenum in [Mo]-N-NH₃¹⁺ is 1.31e, further probing lower electrophilicity of the vanadium complex. This lower exergonic cleavage of the N–N bond with [V] may account for one of the major drawbacks of the [V] catalyst toward NH₃ production.

Three possibilities (Figure 6) exist for the generation of the second equivalent of ammonia and regeneration of the catalyst (the start over of a new cycle). Both experimental^{8a} and theoretical^{8a} reports suggest that different routes for the catalytic cycle are possible. Hence, we have checked three possible pathways of ligand exchange at the end of the cycle, that is, dissociation of NH₃ and addition of N₂. Similar mechanistic possibilities were studied previously by Reiher et al.^{8a} for the [Mo] catalyst with the full HIPT ligand. They concluded that dissociation of the NH₃ ligand may proceed via the neutral pathway or via the anionic one, the latter being the most favorable. As evident from Figure 6, dissociation of NH₃ is favorable via neutral and anionic pathways; the cationic pathway is least likely, while addition of N₂ is most favorable via the

anionic pathway. It is evident from Figure 6 that the reduction of [V]-NH₃¹⁺ to the neutral complex [V]-NH₃ is quite exergonic (–26.7 kcal/mol) with Cp₂Cr* as the reductant, while the subsequent reduction of the neutral complex [V]-NH₃ to the anionic one [V]-NH₃¹⁻ is very unlikely owing to the high endergonic (+74.3 kcal/mol) character of the reaction. Figure 6 reveals that the reduction of [V]-N₂ to [V]-N₂¹⁻ is thermodynamically difficult (the reaction is endergonic by 53.0 kcal/mol). Thus, the reverse of the above reaction, that is, the oxidation of [V]-N₂¹⁻ is thermodynamically favorable. This theoretical finding corroborates experimental finding that {[V]-N₂}K readily undergoes oxidation.^{5k} Further, conversion of [V]-NH₃ to [V]-N₂¹⁻ is thermodynamically unfavorable owing to the high endergonicity associated with the reduction of [V]-NH₃ to [V]-NH₃¹⁻. This may be the cause for the failure in converting [V]-NH₃ into [V]-N₂¹⁻ by the group of Schrock.^{5k}

A closer look at Figure 6 also reveals that the relative ease of dissociation of ammonia, and addition of dinitrogen to the cationic, neutral, and anionic systems follow the order



Thus, the only possible pathway of ligand exchange with [V] catalyst is the neutral one since generation of [V]-NH₃¹⁻ from [V]-NH₃ is thermodynamically quite unfavorable, while both neutral and anionic pathways are viable for [Mo].^{8a} This restriction may also account for the difficult regeneration of the catalyst or start over of a new cycle.

Reiher et al reported that the NH₃/N₂ exchange may also involve associative (addition–elimination) mechanism via the formation of a stable six-coordinate complex [Mo](NH₃)(N₂).^{8c} They could also optimize the six-coordinate complex at the BP86/TZVP-SVP level of theory, and proposed that the course of the reaction could be followed by vibrational frequency analysis (provided that the six-coordinated complex has sufficient lifetime). Hence, we also tried to optimize the six coordinate [V](NH₃)(N₂) complex that should form during the associative mechanism. We tried to attach N₂ from both the top and side entrance, and fully optimized both complexes. However, the optimized geometries obtained from both approaches are the same. We also characterized them to be minima in the potential energy surface by calculating the vibrational frequencies which were found to be all real valued. However, during optimization, we observed that the N₂ ligand moved away from the [V]-NH₃ complex and ultimately attained a distance of 3.551 Å from the vanadium center (see Supporting Information, Figure S2). Interestingly, this distance is larger than the sum of the van der Waals' radii of vanadium and nitrogen (3.34 Å). However, the analogous six-coordinate molybdenum complex has a distance of only 2.285 Å between molybdenum and N₂ which is well within their sum of van der Waals' radii (3.64 Å). It suggests that the formation of the six coordinate intermediate [V](NH₃)(N₂) may not be possible while it is possible for the analogous molybdenum complex as reported by Reiher et al.^{8c} Moreover, the standard free energy of addition of N₂ to [V]-NH₃ is endergonic by 7.8 kcal/mol which is 14.9 kcal/mol higher than the addition of N₂ to the naked “[V]” complex. Thus, the formation of the six coordinate [V](NH₃)(N₂) complex via the addition of N₂ to [V]-NH₃ is thermodynamically unfavorable. Thus, while the associative mechanism may be operative in

case of the molybdenum complex,^{8c} it is less likely to occur with the vanadium catalyst. This might also be a possible reason of the inferiority of the vanadium complex in comparison with the molybdenum complex.

4. CONCLUSIONS

The energy profile for the conversion of N₂ to NH₃ mediated by vanadium triamidoamine has been obtained. This theoretical study corroborates most of the experimental^{5k} findings and is in harmony with previous theoretical studies.^{7,8} The most important steps for the catalytic conversion of N₂ to NH₃ are examined with all the mechanistic possibilities including the possible presence of an activation barrier in the reductive proton migration steps. Our calculation shows that for most of the cases, protonation is more favorable at the amido nitrogen atom than at the terminal one except for the protonation of [V]=N⁻ and [V]-NH₂ where terminal protonation is more favorable for the former and equally favorable for the latter. This is in agreement with previous theoretical and experimental studies.^{8a,21} Some of the key steps of the mechanism were further compared with the well established chemistry of molybdenum.⁶⁻⁸ These key steps include initial reductive proton migration for the process 2 → 3 → 4, N–N bond breaking step, and the ligand exchange step at the end of the cycle. The initial reductive proton migration step with [V] is endergonic by 9.5 kcal/mol while the same process with [Mo] is exergonic by 22.4 kcal/mol. The N–N bond breaking step with [V] is much less exergonic (–4.3 kcal/mol) compared to [Mo] which is highly exergonic (–75.9 kcal/mol). This can be traced to the higher lying $\sigma^*_{Na-N\beta}$ orbital and the lower positive charge at the vanadium center compared with molybdenum of the respective complexes prior to reduction. This lower exergonic character of the N–N bond cleavage step with [V] may account for the lower efficiency of [V] toward NH₃ production.^{5k} The other important step, that is, the ligand exchange step at the end of the cycle reveals that reduction of [V]-NH₃ to [V]-NH₃¹⁻ is very unlikely which corroborates experimental findings.^{5k} Further, the only possible pathway of ligand exchange with [V] is the neutral one, while both anionic and neutral pathways are possible with [Mo]. This restriction provides another clue to the possible limitations of the [V] catalyst. Moreover, the NH₃/N₂ exchange with vanadium is less likely to occur via an associative (addition–elimination) mechanism compared with the analogous molybdenum complex, which might be another possible reason of the inferiority of the vanadium complex in comparison with the molybdenum complex. Thus, we feel that these theoretical findings may help in understanding the possible reasons for the poor performance of vanadium triamidoamine complex toward NH₃ production.

■ ASSOCIATED CONTENT

Supporting Information. Complete citation of ref 16, some additional information, and Cartesian coordinates of the optimized geometries. This material is available free of charge via the Internet at <http://pubs.acs.org>.

■ AUTHOR INFORMATION

Corresponding Author

*Phone: +91 (3712) 267173. Fax: +91 (3712) 267005. E-mail: ashwini@tezu.ernet.in.

■ ACKNOWLEDGMENT

A.K.P. thanks the Department of Science and Technology (DST), New Delhi, for providing financial assistance in the form of a project (project no. DST/FTP/CS-85/2005). A.K.G. thanks Tezpur University for an institutional fellowship. We sincerely thank the reviewers for their critical comments which ultimately helped us in improving the manuscript.

■ REFERENCES

- (1) (a) Burgess, B. K.; Lowe, D. J. *Chem. Rev.* **1996**, *96*, 2983–3012. (b) Hardy, R. W. F.; Bottomly, F.; Burns, R. C. *A Treatise on Dinitrogen Fixation*; Wiley-Interscience: New York, 1979.
- (2) Allen, A. D.; Senoff, C. V. *J. Chem. Soc., Chem. Commun.* **1965**, 621–622.
- (3) Carnahan, J. E.; Mortensen, L. E.; Mower, H. F.; Castle, J. E. *Biochem. Biophys. Acta* **1960**, *38*, 188–189.
- (4) (a) Kim, J.; Rees, D. C. *Science* **1992**, *257*, 1677–1682. (b) Kim, J.; Rees, D. C. *Nature* **1992**, *360*, 553–560.
- (5) (a) Chatt, J.; Leigh, G. J. *Chem. Soc. Rev.* **1972**, *1*, 121–144. (b) Chatt, J.; Dilworth, J. R.; Richards, R. L. *Chem. Rev.* **1978**, *78*, 589–625. (c) Hiday, M.; Mizobe, Y. *Chem. Rev.* **1995**, *95*, 1115–1133. (d) Hiday, M. *Coord. Chem. Rev.* **1999**, *185–186*, 99–108. (e) Pickett, C. J.; Talarmin, J. *Nature* **1985**, *317*, 652–653. (f) George, T. A.; Kovar, R. A. *Inorg. Chem.* **1981**, *20*, 285–287. (g) George, T. A.; Ma, L.; Shailh, S. N.; Tisdale, R. C.; Zubieta, J. *Inorg. Chem.* **1990**, *29*, 4789–4796. (h) George, T. A.; Tisdale, R. C. *Inorg. Chem.* **1988**, *27*, 2909–2912. (i) Fryzuk, M. D.; Kozak, C. M.; Bowdridge, M. R.; Patrick, B. O.; Rettig, S. J. *J. Am. Chem. Soc.* **2002**, *124*, 8389–8397. (j) Mankad, N. P.; Whited, M. T.; Peters, J. C. *Angew. Chem., Int. Ed.* **2007**, *46*, 5768–5771. (k) Smythe, N. C.; Schrock, R. R.; Müller, P.; Weare, W. W. *Inorg. Chem.* **2006**, *45*, 9197–9205. (l) Chu, W.-C.; Wu, C.-C.; Hsu, H.-F. *Inorg. Chem.* **2006**, *45*, 3164–3166. (m) Rees, D. C.; Chan, M. K.; Kim, J. *Adv. Inorg. Chem.* **1993**, *40*, 89–119.
- (6) (a) Yandulov, D. V.; Schrock, R. R. *J. Am. Chem. Soc.* **2002**, *124*, 6252–6253. (b) Yandulov, D. V.; Schrock, R. R. *Science* **2003**, *301*, 76–78. (c) Yandulov, D. V.; Schrock, R. R. *Inorg. Chem.* **2005**, *44*, 1103–1117. (d) Yandulov, D. V.; Schrock, R. R.; Rheingold, A. L.; Ceccarelli, C.; Davis, W. M. *Inorg. Chem.* **2003**, *42*, 796–813. (e) Ritleng, V.; Yandulov, D. V.; Weare, W. W.; Schrock, R. R.; Hock, A. S.; Davis, W. M. *J. Am. Chem. Soc.* **2004**, *126*, 6150–6163. (f) Schrock, R. R. *Angew. Chem., Int. Ed.* **2008**, *47*, 5512–5522.
- (7) (a) Studt, F.; Tuzcek, F. *Angew. Chem., Int. Ed.* **2005**, *44*, 5639–5642. (b) Mersmann, K.; Horn, K. H.; Böres, N.; Lehnert, N.; Studt, F.; Paulat, F.; Peters, G.; Burmazovic, I. I.; Eldik, R. v.; Tuzcek, F. *Inorg. Chem.* **2005**, *44*, 3031–3045. (c) Studt, F.; Tuzcek, F. *J. Comput. Chem.* **2006**, *27*, 1278–1291. (d) Stephan, G. C.; Sivasankar, C.; Studt, F.; Tuzcek, F. *Chem.—Eur. J.* **2008**, *14*, 644–652.
- (8) (a) Reiher, M.; Guennic, B. L.; Kirchner, B. *Inorg. Chem.* **2005**, *44*, 9640–9642. (b) Schenk, S.; Guennic, B. L.; Kirchner, B.; Reiher, M. *Inorg. Chem.* **2008**, *47*, 3634–3650. (c) Schenk, S.; Kirchner, B.; Reiher, M. *Chem.—Eur. J.* **2009**, *15*, 5073–5082. (d) Cao, Z.; Zhou, Z.; Wan, H.; Zhang, Q. *Int. J. Quantum Chem.* **2005**, *103*, 344–353. (e) Neese, F. *Angew. Chem., Int. Ed.* **2005**, *44*, 2–6. (f) Hölscher, M.; Leitner, W. *Eur. J. Inorg. Chem.* **2006**, 4407. (g) Khoroshun, D. V.; Musaev, D. G.; Morokuma, K. *Mol. Phys.* **2002**, *100*, 523.
- (9) Eady, R. R. *Chem. Rev.* **1996**, *96*, 3013–3030.
- (10) Guha, A. K.; Phukan, A. K. *Inorg. Chim. Acta* **2010**, *363*, 3270–3273.
- (11) (a) Ehlers, A. W.; Frenking, G. *J. Am. Chem. Soc.* **1994**, *116*, 1514–1520. (b) Delley, B.; Wrinn, M.; Lüthi, H. P. *J. Chem. Phys.* **1994**, *100*, 5785–5791. (c) Barckholtz, T. A.; Bursten, B. E. *J. Am. Chem. Soc.* **1998**, *120*, 1926–1927. (d) Niu, S.; Hall, M. B. *Chem. Rev.* **2000**, *100*, 353–406. (e) Ziegler, T.; Autschbach, J. *Chem. Rev.* **2005**, *105*, 2695–2722.
- (12) Perdew, J. P.; Burke, K.; Ernzerhof, M. *Phys. Rev. Lett.* **1996**, *77*, 3865–3868.

(13) (a) Grimme, S. *J. Phys. Chem. A* **2005**, *109*, 3067–3077.
(b) Bühl, M.; Reimann, C.; Pantazis, D. A.; Bresow, T.; Neese, F. *J. Chem. Theory Comput.* **2008**, *4*, 1449–1459.

(14) (a) Dolg, M.; Wedig, U.; Stoll, H.; Preuss, H. *J. Chem. Phys.* **1987**, *86*, 866–872. (b) Dunning, T. H., Jr.; Hay, P. J. In *Modern Theoretical Chemistry*; Schaefer, H. F., III, Ed.; Plenum: New York, 1976; Vol. 3, pp 1–28.

(15) (a) Reed, A. E.; Weinhold, F. *J. Chem. Phys.* **1983**, *78*, 4066–4073. (b) Reed, A. E.; Weinstock, R. B.; Weinhold, F. *J. Chem. Phys.* **1985**, *83*, 735–647. (c) Reed, A. E.; Curtiss, L. A.; Weinhold, F. *Chem. Rev.* **1988**, *88*, 899–926.

(16) Frisch, M. C. et al. *Gaussian 03*, revision D.01; Gaussian, Inc.: Wallingford, CT, 2004; For the complete reference, see the Supporting Information.

(17) Dapprich, S.; Frenking, G. *J. Phys. Chem.* **1995**, *99*, 9352–9362.

(18) (a) Tenderholt, A. L. *QMForge*, Version 2.1; <http://qmforge.sourceforge.net>. (b) O'Boyle, N. M.; Tenderholt, A. L.; Langner, K. M. *J. Comput. Chem.* **2008**, *29*, 839–845.

(19) (a) Dewar, M. J. S. *Bull. Soc. Chim. Fr.* **1951**, *18*, C71–79.

(b) Chatt, J.; Duncanson, L. A. *J. Chem. Soc.* **1953**, 2939–2947.

(20) (a) Fryzuk, M. D.; Johnson, S. A. *Coord. Chem. Rev.* **2000**, *200–202*, 379–409. (b) Hazari, N. *Chem. Soc. Rev.* **2010**, *39*, 4044–4056.

(21) Kinney, R. A.; McNaughton, R. L.; Chin, J. M.; Schrock, R. R.; Hoffman, B. M. *Inorg. Chem.* **2011**, *50*, 418–420.

(22) Huheey, J. E.; Keiter, E. A.; Keiter, R. L. *Inorganic Chemistry: Principles of Structure and Reactivity*, 4th ed.; Pearson Education Pte. Ltd.: Singapore, 2004.